Electronic Supplementary Material (ESI) for Analyst.

Supporting information

Colorimetric Identification of Lanthanide Ions Based on Two Carboxylic Acids as an Artificial Tongue

Chi Zhang,[1] Juan Huang,[1] Wei Wei,[2]*Zhengbo Chen[1]*

[1]Department of Chemistry, Capital Normal University, Beijing, 100048, China

[2]School of Chemistry and Chemical Engineering, Shangqiu Normal University, Shangqiu, 476000, China

E-mail: weiweizzuli@163.com; czb979216@sina.com

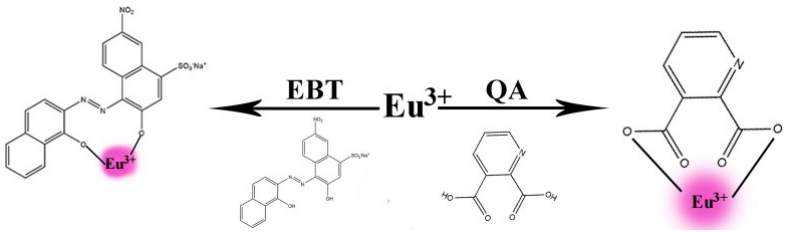

Fig. S1 The interaction mode between lanthanide ions and EBT, and between lanthanide ions and the carboxylic acids.

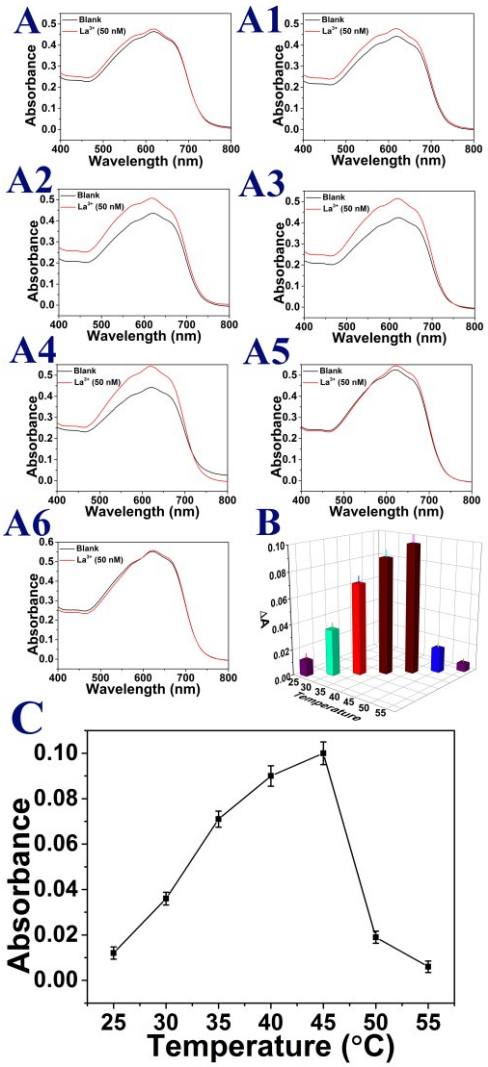

Fig. S2 UV-vis spectra of EBT (2 μM)-QA (100 nM)-La^{3+} (10 nM) solutions at different temperatures. (A) 25 °C, (A1) 30 °C, (A2) 35 °C, (A3) 40 °C, (A4) 45 °C, (A5) 50 °C, (A6) 55 °C. (B,C) Change of absorbance of EBT at 615 nm at different temperatures.

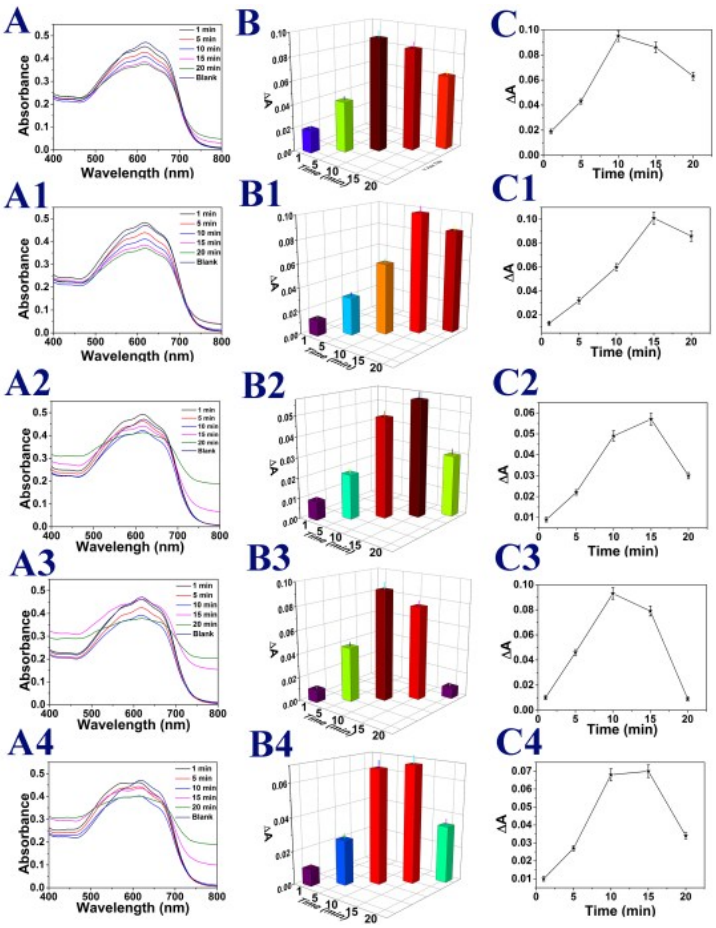

Fig. S3 (A-A4) UV-vis spectra of EBT (2 μM)-QA (100 nM)-lanthanide ion (10 nM) solutions at different incubation time. (B-B4,C-C4) Change of absorbance of EBT at 615 nm at different incubation time. (A,B,C) La^{3+}, (A1,B1,C1) Sm^{3+}, (A2,B2,C2) Eu^{3+}, (A3,B3,C3) Gd^{3+}, (A4,B4,C4)Yb^{3+}.

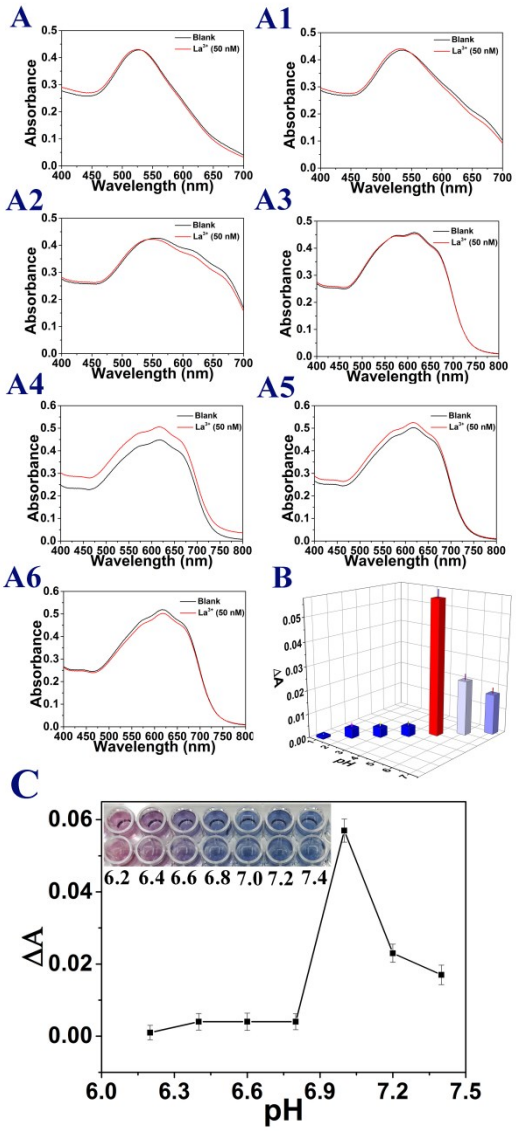

Fig. S4 (A-A6) UV-vis spectra of EBT (2 μM)-QA (100 nM)-La^{3+} (10 nM) solutions at different pH values: (A) 6.2, (A1) 6.4, (A2) 6.6, (A3) 6.8, (A4) 7.0, (A5) 7.2, (A6) 7.4. (B,C) Change of absorbance of EBT at 615 nm in different pH of solutions.

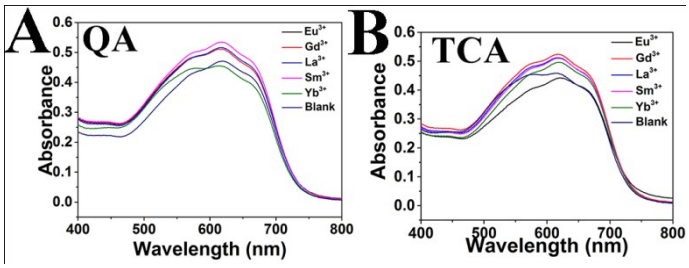

Fig. S5 The UV-vis absorption spectra of (A) QA, and (B) TCA before and after addition of different lanthanide ions at 10 nM.

Table S1 Basic properties of the carboxylic acids in the experiment

Reagents	Abbreviation	Molecular weight	Structure
Quinolinic acid	QA	167.12	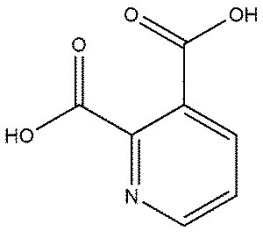
Tannic acid	TCA	1701.2	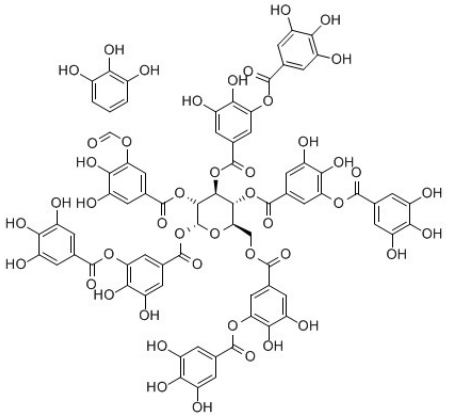

Table S2 The training matrix of the colorimetric response patterns against 5 lanthanide ions by using this sensor assay at the concentration of 500 nM.

Lanthanide ions	$A_i–A_0$ (QA)	$A_i–A_0$ (TCA)
La^{3+}	0.015	-0.014
La^{3+}	0.019	-0.011
La^{3+}	0.012	-0.01
La^{3+}	0.014	-0.014
La^{3+}	0.014	-0.012
Sm^{3+}	0.03	0.04
Sm^{3+}	0.034	0.043
Sm^{3+}	0.027	0.044
Sm^{3+}	0.03	0.04
Sm^{3+}	0.031	0.042
Eu^{3+}	0.014	0.036
Eu^{3+}	0.017	0.038
Eu^{3+}	0.012	0.039
Eu^{3+}	0.015	0.036
Eu^{3+}	0.016	0.038
Gd^{3+}	0.024	0.034
Gd^{3+}	0.028	0.036
Gd^{3+}	0.023	0.037
Gd^{3+}	0.025	0.034
Gd^{3+}	0.026	0.036
Yb^{3+}	0.029	0.042
Yb^{3+}	0.032	0.044
Yb^{3+}	0.027	0.045
Yb^{3+}	0.029	0.042
Yb^{3+}	0.031	0.044

Table S3 The training matrix of the colorimetric response patterns against 5 lanthanide ions by using this sensor assay at the concentration of 400 nM.

Lanthanide ions	$A_i–A_0$ (QA)	$A_i–A_0$ (TCA)
La^{3+}	0.024	0.041
La^{3+}	0.028	0.046
La^{3+}	0.022	0.043
La^{3+}	0.025	0.04
La^{3+}	0.026	0.042
Sm^{3+}	0.015	0.053
Sm^{3+}	0.019	0.056
Sm^{3+}	0.012	0.057
Sm^{3+}	0.016	0.053
Sm^{3+}	0.016	0.055
Eu^{3+}	0.036	0.056
Eu^{3+}	0.039	0.057
Eu^{3+}	0.034	0.059
Eu^{3+}	0.036	0.057
Eu^{3+}	0.037	0.06
Gd^{3+}	0.031	0.047
Gd^{3+}	0.033	0.051
Gd^{3+}	0.029	0.051
Gd^{3+}	0.03	0.048
Gd^{3+}	0.031	0.049
Yb^{3+}	0.03	0.084
Yb^{3+}	0.033	0.085
Yb^{3+}	0.028	0.088
Yb^{3+}	0.03	0.083
Yb^{3+}	0.031	0.086

Table S4 The training matrix of the colorimetric response patterns against 5 lanthanide ions by using this sensor assay at the concentration of 300 nM.

Lanthanide ions	$A_i–A_0$ (QA)	$A_i–A_0$ (TCA)
La^{3+}	0.005	0.027
La^{3+}	0.008	0.03
La^{3+}	0.002	0.031
La^{3+}	0.005	0.026
La^{3+}	0.005	0.028
Sm^{3+}	0.016	0.06
Sm^{3+}	0.02	0.062
Sm^{3+}	0.013	0.063
Sm^{3+}	0.017	0.059
Sm^{3+}	0.017	0.061
Eu^{3+}	0.043	0.05
Eu^{3+}	0.048	0.052
Eu^{3+}	0.041	0.053
Eu^{3+}	0.045	0.049
Eu^{3+}	0.046	0.051
Gd^{3+}	0.014	0.048
Gd^{3+}	0.018	0.051
Gd^{3+}	0.012	0.052
Gd^{3+}	0.015	0.047
Gd^{3+}	0.016	0.049
Yb^{3+}	0.026	0.056
Yb^{3+}	0.029	0.058
Yb^{3+}	0.023	0.058
Yb^{3+}	0.026	0.054
Yb^{3+}	0.027	0.056

Table S5 The training matrix of the colorimetric response patterns against 5 lanthanide ions by using this sensor assay at the concentration of 200 nM.

Lanthanide ions	$A_i–A_0$ (QA)	$A_i–A_0$ (TCA)
La^{3+}	-0.031	-0.008
La^{3+}	-0.028	-0.006
La^{3+}	-0.03	-0.006
La^{3+}	-0.031	-0.011
La^{3+}	-0.03	-0.01
Sm^{3+}	-0.014	0.006
Sm^{3+}	-0.012	0.008
Sm^{3+}	-0.019	0.009
Sm^{3+}	-0.016	0.005
Sm^{3+}	-0.015	0.007
Eu^{3+}	0.002	0.027
Eu^{3+}	0.005	0.032
Eu^{3+}	-0.002	0.03
Eu^{3+}	0.001	0.026
Eu^{3+}	0.002	0.028
Gd^{3+}	-0.021	0.006
Gd^{3+}	-0.02	0.006
Gd^{3+}	-0.027	0.007
Gd^{3+}	-0.024	0.002
Gd^{3+}	-0.023	0.005
Yb^{3+}	-0.015	0.011
Yb^{3+}	-0.016	0.015
Yb^{3+}	-0.022	0.015
Yb^{3+}	-0.019	0.011
Yb^{3+}	-0.019	0.012

Table S6 The training matrix of the colorimetric response patterns against 5lanthanide ions by using this sensor assay at the concentration of 100 nM.

Lanthanide ions	A_i–A_0 (QA)	A_i–A_0 (TCA)
La^{3+}	-0.052	-0.012
La^{3+}	-0.048	-0.01
La^{3+}	-0.055	-0.01
La^{3+}	-0.053	-0.013
La^{3+}	-0.05	-0.012
Sm^{3+}	-0.037	-0.01
Sm^{3+}	-0.033	-0.007
Sm^{3+}	-0.04	-0.005
Sm^{3+}	-0.037	-0.008
Sm^{3+}	-0.035	-0.008
Eu^{3+}	-0.015	-0.008
Eu^{3+}	-0.014	-0.005
Eu^{3+}	-0.016	-0.006
Eu^{3+}	-0.016	-0.006
Eu^{3+}	-0.015	-0.006
Gd^{3+}	-0.024	-0.021
Gd^{3+}	-0.02	-0.019
Gd^{3+}	-0.027	-0.018
Gd^{3+}	-0.024	-0.022
Gd^{3+}	-0.023	-0.019
Yb^{3+}	-0.005	0.012
Yb^{3+}	-0.002	0.015
Yb^{3+}	-0.008	0.016
Yb^{3+}	-0.005	0.013
Yb^{3+}	-0.005	0.014

Table S7 The training matrix of the colorimetric response patterns against 5 lanthanide ions by using this sensor assay at the concentration of 50 nM.

Lanthanide ions	$A_i–A_0$ (QA)	$A_i–A_0$ (TCA)
La^{3+}	-0.045	-0.007
La^{3+}	-0.041	-0.007
La^{3+}	-0.046	-0.003
La^{3+}	-0.042	-0.006
La^{3+}	-0.04	-0.008
Sm^{3+}	-0.064	0.015
Sm^{3+}	-0.059	0.02
Sm^{3+}	-0.066	0.023
Sm^{3+}	-0.062	0.022
Sm^{3+}	-0.058	0.025
Eu^{3+}	-0.019	-0.013
Eu^{3+}	-0.018	-0.015
Eu^{3+}	-0.021	-0.005
Eu^{3+}	-0.019	-0.011
Eu^{3+}	-0.019	-0.012
Gd^{3+}	-0.035	0.002
Gd^{3+}	-0.033	0.004
Gd^{3+}	-0.038	0.009
Gd^{3+}	-0.036	0.005
Gd^{3+}	-0.034	0.005
Yb^{3+}	0.036	0.073
Yb^{3+}	0.046	0.077
Yb^{3+}	0.04	0.085
Yb^{3+}	0.04	0.098
Yb^{3+}	0.04	0.093

Table S8 The training matrix of the colorimetric response patterns against 5 lanthanide ions by using this sensor assay at the concentration of 10 nM.

Lanthanide ions	A_i–A_0 (QA)	A_i–A_0 (TCA)
La^{3+}	0.007	0.013
La^{3+}	0.006	0.013
La^{3+}	0.005	0.014
La^{3+}	0.006	0.013
La^{3+}	0.005	0.012
Sm^{3+}	-0.001	0.001
Sm^{3+}	-0.003	0.002
Sm^{3+}	-0.003	0.002
Sm^{3+}	-0.003	0.002
Sm^{3+}	-0.003	0.002
Eu^{3+}	0.012	0.016
Eu^{3+}	0.01	0.016
Eu^{3+}	0.01	0.016
Eu^{3+}	0.01	0.016
Eu^{3+}	0.01	0.016
Gd^{3+}	0.019	0.013
Gd^{3+}	0.016	0.012
Gd^{3+}	0.016	0.012
Gd^{3+}	0.016	0.013
Gd^{3+}	0.016	0.012
Yb^{3+}	0.016	0.022
Yb^{3+}	0.014	0.022
Yb^{3+}	0.014	0.022
Yb^{3+}	0.014	0.021
Yb^{3+}	0.014	0.021

Table S9 The training matrix of the colorimetric response patterns against La^{3+} at different concentrations by using this sensor assay.

Lanthanide ions	$A_i–A_0$ (QA)	$A_i–A_0$ (TCA)
50 nM	-0.045	-0.007
50 nM	-0.041	-0.007
50 nM	-0.046	-0.003
50 nM	-0.042	-0.006
50 nM	-0.04	-0.008
100 nM	-0.052	-0.012
100 nM	-0.048	-0.01
100 nM	-0.055	-0.01
100 nM	-0.053	-0.013
100 nM	-0.05	-0.012
200 nM	-0.031	-0.008
200 nM	-0.028	-0.006
200 nM	-0.03	-0.006
200 nM	-0.031	-0.011
200 nM	-0.03	-0.01
300 nM	0.005	0.027
300 nM	0.008	0.03
300 nM	0.002	0.031
300 nM	0.005	0.026
300 nM	0.005	0.028
400 nM	0.024	0.041
400 nM	0.028	0.046
400 nM	0.022	0.043
400 nM	0.025	0.04
400 nM	0.026	0.042

Table S10 The training matrix of the colorimetric response patterns against Sm^{3+} at different concentrations by using this sensor assay.

Lanthanide ions	$A_i–A_0$ (QA)	$A_i–A_0$ (TCA)
50 nM	-0.064	0.015
50 nM	-0.059	0.02
50 nM	-0.066	0.023
50 nM	-0.062	0.022
50 nM	-0.058	0.025
100 nM	-0.037	-0.01
100 nM	-0.033	-0.007
100 nM	-0.04	-0.005
100 nM	-0.037	-0.008
100 nM	-0.035	-0.008
200 nM	-0.014	0.006
200 nM	-0.012	0.008
200 nM	-0.019	0.009
200 nM	-0.016	0.005
200 nM	-0.015	0.007
300 nM	0.016	0.06
300 nM	0.02	0.062
300 nM	0.013	0.063
300 nM	0.017	0.059
300 nM	0.017	0.061
500 nM	0.03	0.04
500 nM	0.034	0.043
500 nM	0.027	0.044
500 nM	0.03	0.04
500 nM	0.031	0.042

Table S11 The training matrix of the colorimetric response patterns against Eu^{3+} at different concentrations by using this sensor assay.

Lanthanide ions	A_i–A_0 (QA)	A_i–A_0 (TCA)
50 nM	-0.118	0
50 nM	-0.118	0
50 nM	-0.117	0.028
50 nM	-0.117	-0.028
50 nM	-0.116	0.028
100 nM	-0.135	0
100 nM	-0.137	0.055
100 nM	-0.136	0
100 nM	-0.136	-0.028
100 nM	-0.137	0.028
200 nM	-0.163	0
200 nM	-0.164	0
200 nM	-0.165	0.028
200 nM	-0.164	-0.055
200 nM	-0.163	0
300 nM	-0.189	-0.052
300 nM	-0.191	0
300 nM	-0.188	-0.027
300 nM	-0.19	0.045
300 nM	-0.192	-0.03
400 nM	-0.214	-0.027
400 nM	-0.216	0.013
400 nM	-0.215	-0.027
400 nM	-0.215	-0.042
400 nM	-0.217	-0.04

Table S12 The training matrix of the colorimetric response patterns against Gd^{3+} at different concentrations by using this sensor assay.

Lanthanide ions	$A_i–A_0$ (QA)	$A_i–A_0$ (TCA)
50 nM	-0.035	0.002
50 nM	-0.033	0.004
50 nM	-0.038	0.009
50 nM	-0.036	0.005
50 nM	-0.034	0.005
100 nM	-0.024	-0.021
100 nM	-0.02	-0.019
100 nM	-0.027	-0.018
100 nM	-0.024	-0.022
100 nM	-0.023	-0.019
200 nM	-0.021	0.006
200 nM	-0.02	0.006
200 nM	-0.027	0.007
200 nM	-0.024	0.002
200 nM	-0.023	0.005
300 nM	0.014	0.048
300 nM	0.018	0.051
300 nM	0.012	0.052
300 nM	0.015	0.047
300 nM	0.016	0.049
400 nM	0.031	0.047
400 nM	0.033	0.051
400 nM	0.029	0.051
400 nM	0.03	0.048
400 nM	0.031	0.049

Table S13 The training matrix of the colorimetric response patterns against Yb^{3+} at different concentrations by using this sensor assay.

Lanthanide ions	$A_i–A_0$ (QA)	$A_i–A_0$ (TCA)
100 nM	-0.005	0.012
100 nM	-0.002	0.015
100 nM	-0.008	0.016
100 nM	-0.005	0.013
100 nM	-0.005	0.014
200 nM	-0.015	0.011
200 nM	-0.016	0.015
200 nM	-0.022	0.015
200 nM	-0.019	0.011
200 nM	-0.019	0.012
300 nM	0.026	0.056
300 nM	0.029	0.058
300 nM	0.023	0.058
300 nM	0.026	0.054
300 nM	0.027	0.056
400 nM	0.03	0.084
400 nM	0.033	0.085
400 nM	0.028	0.088
400 nM	0.03	0.083
400 nM	0.031	0.086
500 nM	0.029	0.042
500 nM	0.032	0.044
500 nM	0.027	0.045
500 nM	0.029	0.042
500 nM	0.031	0.044

Table S14 The training matrix of the colorimetric response patterns against the mixturesof Lanthanide ions at 10 nM by using this sensor assay.

Lanthanide ions	$A_i–A_0$ (QA)	$A_i–A_0$ (TCA)
La^{3+}:Sm^{3+}=1:2	-0.0014	-0.106
La^{3+}:Sm^{3+}=1:2	-0.0028	-0.1065
La^{3+}:Sm^{3+}=1:2	-0.0011	-0.104
La^{3+}:Sm^{3+}=1:2	-0.002	-0.102
La^{3+}:Sm^{3+}=1:2	-0.0008	-0.0994
La^{3+}:Eu^{3+}=3:7	0.0156	-0.1876
La^{3+}:Eu^{3+}=3:7	0.0144	-0.1844
La^{3+}:Eu^{3+}=3:7	0.0159	-0.1869
La^{3+}:Eu^{3+}=3:7	0.0155	-0.1821
La^{3+}:Eu^{3+}=3:7	0.0169	-0.1871
Gd^{3+}:Yb^{3+}=4:6	-0.0113	-0.2582
Gd^{3+}:Yb^{3+}=4:6	-0.0124	-0.2592
Gd^{3+}:Yb^{3+}=4:6	-0.0107	-0.2616
Gd^{3+}:Yb^{3+}=4:6	-0.0103	-0.2609
Gd^{3+}:Yb^{3+}=4:6	-0.0088	-0.2658
Sm^{3+}:Yb^{3+}=5:5	-0.007	-0.0445
Sm^{3+}:Yb^{3+}=5:5	-0.0096	-0.0413
Sm^{3+}:Yb^{3+}=5:5	-0.0086	-0.0381
Sm^{3+}:Yb^{3+}=5:5	-0.0095	-0.032
Sm^{3+}:Yb^{3+}=5:5	-0.0086	-0.0325
La^{3+}:Gd^{3+}:Yb^{3+}=3:3:4	0.0038	-0.0213
La^{3+}:Gd^{3+}:Yb^{3+}=3:3:4	0.0019	-0.021
La^{3+}:Gd^{3+}:Yb^{3+}=3:3:4	0.0029	-0.0203
La^{3+}:Gd^{3+}:Yb^{3+}=3:3:4	0.0021	-0.0143
La^{3+}:Gd^{3+}:Yb^{3+}=3:3:4	0.0027	-0.0183
La^{3+}:Sm^{3+}:Eu^{3+}:Gd^{3+}=1:2:3:4	0.0024	-0.1451
La^{3+}:Sm^{3+}:Eu^{3+}:Gd^{3+}=1:2:3:4	0.0022	-0.1442
La^{3+}:Sm^{3+}:Eu^{3+}:Gd^{3+}=1:2:3:4	0.0023	-0.1416
La^{3+}:Sm^{3+}:Eu^{3+}:Gd^{3+}=1:2:3:4	0.0039	-0.1441
La^{3+}:Sm^{3+}:Eu^{3+}:Gd^{3+}=1:2:3:4	0.0042	-0.1414

Table S15 The training matrix of the colorimetric response patterns againstthe lanthanide ions at different concentrations by using this sensor assay.

Lanthanide ions	$A_i–A_0$ (QA)	$A_i–A_0$ (TCA)
La^{3+}(500nM)	0.015	-0.014
La^{3+}(500nM)	0.019	-0.011
La^{3+}(500nM)	0.012	-0.01
La^{3+}(500nM)	0.014	-0.014
La^{3+}(500nM)	0.014	-0.012
La^{3+}(200nM)	-0.031	-0.008
La^{3+}(200nM)	-0.028	-0.006
La^{3+}(200nM)	-0.03	-0.006
La^{3+}(200nM)	-0.031	-0.011
La^{3+}(200nM)	-0.03	-0.01
La^{3+}(100nM)	-0.052	-0.012
La^{3+}(100nM)	-0.048	-0.01
La^{3+}(100nM)	-0.055	-0.01
La^{3+}(100nM)	-0.053	-0.013
La^{3+}(100nM)	-0.05	-0.012
La^{3+}(50nM)	-0.045	-0.007
La^{3+}(50nM)	-0.041	-0.007
La^{3+}(50nM)	-0.046	-0.003
La^{3+}(50nM)	-0.042	-0.006
La^{3+}(50nM)	-0.04	-0.008
La^{3+}(10nM)	0.007	0.013
La^{3+}(10nM)	0.006	0.013
La^{3+}(10nM)	0.005	0.014
La^{3+}(10nM)	0.006	0.013
La^{3+}(10nM)	0.005	0.012
Sm^{3+}(50nM)	-0.064	0.015
Sm^{3+}(50nM)	-0.059	0.02
Sm^{3+}(50nM)	-0.066	0.023
Sm^{3+}(50nM)	-0.062	0.022
Sm^{3+}(50nM)	-0.058	0.025
Sm^{3+}(10nM)	-0.001	0.001
Sm^{3+}(10nM)	-0.003	0.002
Sm^{3+}(10nM)	-0.003	0.002
Sm^{3+}(10nM)	-0.003	0.002
Sm^{3+}(10nM)	-0.003	0.002
Eu^{3+}(500nM)	0.014	0.036
Eu^{3+}(500nM)	0.017	0.038
Eu^{3+}(500nM)	0.012	0.039
Eu^{3+}(500nM)	0.015	0.036
Eu^{3+}(500nM)	0.016	0.038
Eu^{3+}(100nM)	-0.015	-0.008

Eu^{3+}(100nM)	-0.014	-0.005
Eu^{3+}(100nM)	-0.016	-0.006
Eu^{3+}(100nM)	-0.016	-0.006
Eu^{3+}(100nM)	-0.015	-0.006
Eu^{3+}(10nM)	0.012	0.016
Eu^{3+}(10nM)	0.01	0.016
Eu^{3+}(10nM)	0.01	0.016
Eu^{3+}(10nM)	0.01	0.016
Eu^{3+}(10nM)	0.01	0.016
Gd^{3+}(500nM)	0.024	0.034
Gd^{3+}(500nM)	0.028	0.036
Gd^{3+}(500nM)	0.023	0.037
Gd^{3+}(500nM)	0.025	0.034
Gd^{3+}(500nM)	0.026	0.036
Gd^{3+}(200nM)	-0.021	0.006
Gd^{3+}(200nM)	-0.02	0.006
Gd^{3+}(200nM)	-0.027	0.007
Gd^{3+}(200nM)	-0.024	0.002
Gd^{3+}(200nM)	-0.023	0.005
Gd^{3+}(100nM)	-0.024	-0.021
Gd^{3+}(100nM)	-0.02	-0.019
Gd^{3+}(100nM)	-0.027	-0.018
Gd^{3+}(100nM)	-0.024	-0.022
Gd^{3+}(100nM)	-0.023	-0.019
Gd^{3+}(50nM)	-0.035	0.002
Gd^{3+}(50nM)	-0.033	0.004
Gd^{3+}(50nM)	-0.038	0.009
Gd^{3+}(50nM)	-0.036	0.005
Gd^{3+}(50nM)	-0.034	0.005
Gd^{3+}(10nM)	0.019	0.013
Gd^{3+}(10nM)	0.016	0.012
Gd^{3+}(10nM)	0.016	0.012
Gd^{3+}(10nM)	0.016	0.013
Gd^{3+}(10nM)	0.016	0.012
Yb^{3+}(400nM)	0.03	0.084
Yb^{3+}(400nM)	0.033	0.085
Yb^{3+}(400nM)	0.028	0.088
Yb^{3+}(400nM)	0.03	0.083
Yb^{3+}(400nM)	0.031	0.086
Yb^{3+}(100nM)	-0.005	0.012
Yb^{3+}(100nM)	-0.002	0.015
Yb^{3+}(100nM)	-0.008	0.016
Yb^{3+}(100nM)	-0.005	0.013
Yb^{3+}(100nM)	-0.005	0.014

Yb^{3+}(10nM)	0.016	0.022
Yb^{3+}(10nM)	0.014	0.022
Yb^{3+}(10nM)	0.014	0.022
Yb^{3+}(10nM)	0.014	0.021
Yb^{3+}(10nM)	0.014	0.021

Table S16. The training matrix of the colorimetric response patterns against the 5 lanthanide ions at 10 nM with Ag^{+},Pb^{2+},Hg^{2+},Fe^{3+},and Cd^{3+}at 100 nM as potential interferences using this sensor assay.

Lanthanide ions	A_i–A_0 (QA)	A_i–A_0 (TCA)
La^{3+}	0.007	0.013
La^{3+}	0.006	0.013
La^{3+}	0.005	0.014
La^{3+}	0.006	0.013
La^{3+}	0.005	0.012
Sm^{3+}	-0.001	0.001
Sm^{3+}	-0.003	0.002
Sm^{3+}	-0.003	0.002
Sm^{3+}	-0.003	0.002
Sm^{3+}	-0.003	0.002
Eu^{3+}	0.012	0.016
Eu^{3+}	0.01	0.016
Eu^{3+}	0.01	0.016
Eu^{3+}	0.01	0.016
Eu^{3+}	0.01	0.016
Gd^{3+}	0.019	0.013
Gd^{3+}	0.016	0.012
Gd^{3+}	0.016	0.012
Gd^{3+}	0.016	0.013
Gd^{3+}	0.016	0.012
Yb^{3+}	0.016	0.022
Yb^{3+}	0.014	0.022
Yb^{3+}	0.014	0.022
Yb^{3+}	0.014	0.021
Yb^{3+}	0.014	0.021
Ag^{+}	0.001	-0.004
Ag^{+}	-0.001	-0.003
Ag^{+}	0	-0.004
Ag^{+}	-0.001	-0.003
Ag^{+}	-0.001	-0.004
Pb^{2+}	0.174	0.141
Pb^{2+}	0.17	0.141
Pb^{2+}	0.171	0.141
Pb^{2+}	0.171	0.141
Pb^{2+}	0.17	0.141
Hg^{2+}	0.011	-0.006
Hg^{2+}	0.009	-0.005
Hg^{2+}	0.009	-0.005
Hg^{2+}	0.009	-0.005

Hg^{2+}	0.009	-0.005
Fe^{3+}	0.176	0.146
Fe^{3+}	0.174	0.149
Fe^{3+}	0.173	0.148
Fe^{3+}	0.173	0.149
Fe^{3+}	0.173	0.148
Cd^{3+}	0.182	0.173
Cd^{3+}	0.18	0.174
Cd^{3+}	0.181	0.174
Cd^{3+}	0.18	0.174
Cd^{3+}	0.181	0.174

Table S17 The training matrix of the colorimetric response patterns against the 5 Lanthanide ions at 300 nM in river samples by using this sensor assay.

Lanthanide ions	$A_i–A_0$ (QA)	$A_i–A_0$ (TCA)
La^{3+}	0.047	0.062
La^{3+}	0.042	0.063
La^{3+}	0.047	0.065
La^{3+}	0.047	0.064
La^{3+}	0.048	0.065
Sm^{3+}	0.085	0.096
Sm^{3+}	0.086	0.095
Sm^{3+}	0.088	0.097
Sm^{3+}	0.086	0.097
Sm^{3+}	0.087	0.098
Eu^{3+}	0.125	0.139
Eu^{3+}	0.124	0.14
Eu^{3+}	0.127	0.14
Eu^{3+}	0.126	0.141
Eu^{3+}	0.127	0.142
Gd^{3+}	0.084	0.111
Gd^{3+}	0.082	0.108
Gd^{3+}	0.084	0.105
Gd^{3+}	0.084	0.106
Gd^{3+}	0.085	0.107
Yb^{3+}	0.091	0.068
Yb^{3+}	0.087	0.071
Yb^{3+}	0.088	0.073
Yb^{3+}	0.086	0.074
Yb^{3+}	0.087	0.075

Table S18 The training matrix of the colorimetric response patterns against the 5 Lanthanide ions at 200 nM in river samples by using this sensor assay.

Lanthanide ions	A_i–A_0 (QA)	A_i–A_0 (TCA)
La^{3+}	0.029	0.046
La^{3+}	0.029	0.045
La^{3+}	0.03	0.044
La^{3+}	0.029	0.045
La^{3+}	0.03	0.046
Sm^{3+}	0.051	0.071
Sm^{3+}	0.049	0.075
Sm^{3+}	0.049	0.075
Sm^{3+}	0.05	0.074
Sm^{3+}	0.05	0.075
Eu^{3+}	0.059	0.092
Eu^{3+}	0.057	0.092
Eu^{3+}	0.057	0.092
Eu^{3+}	0.058	0.093
Eu^{3+}	0.058	0.093
Gd^{3+}	0.029	0.076
Gd^{3+}	0.027	0.077
Gd^{3+}	0.027	0.076
Gd^{3+}	0.028	0.077
Gd^{3+}	0.027	0.078
Yb^{3+}	0.055	0.079
Yb^{3+}	0.053	0.081
Yb^{3+}	0.053	0.079
Yb^{3+}	0.054	0.081
Yb^{3+}	0.053	0.082

Table S19 The training matrix of the colorimetric response patterns against the 5 Lanthanide ions at 100 nM in river samples by using this sensor assay.

Lanthanide ions	A_i–A_0 (QA)	A_i–A_0 (TCA)
La^{3+}	0.065	0.074
La^{3+}	0.064	0.078
La^{3+}	0.063	0.079
La^{3+}	0.064	0.079
La^{3+}	0.063	0.076
Sm^{3+}	0.08	0.106
Sm^{3+}	0.083	0.109
Sm^{3+}	0.082	0.11
Sm^{3+}	0.083	0.111
Sm^{3+}	0.082	0.108
Eu^{3+}	0.09	0.103
Eu^{3+}	0.093	0.107
Eu^{3+}	0.091	0.107
Eu^{3+}	0.094	0.108
Eu^{3+}	0.091	0.105
Gd^{3+}	0.085	0.108
Gd^{3+}	0.088	0.111
Gd^{3+}	0.086	0.112
Gd^{3+}	0.089	0.113
Gd^{3+}	0.087	0.11
Yb^{3+}	0.077	0.081
Yb^{3+}	0.081	0.085
Yb^{3+}	0.08	0.085
Yb^{3+}	0.082	0.086
Yb^{3+}	0.081	0.083

Table S20 The training matrix of the colorimetric response patterns against the 5 Lanthanide ions at 50 nM in river samples by using this sensor assay.

Lanthanide ions	$A_i–A_0$ (QA)	$A_i–A_0$ (TCA)
La^{3+}	0.029	0.061
La^{3+}	0.029	0.06
La^{3+}	0.029	0.061
La^{3+}	0.03	0.061
La^{3+}	0.01	0.057
Sm^{3+}	0.011	0.058
Sm^{3+}	0.011	0.059
Sm^{3+}	0.011	0.059
Sm^{3+}	0.011	0.059
Sm^{3+}	0.084	0.079
Eu^{3+}	0.084	0.079
Eu^{3+}	0.085	0.08
Eu^{3+}	0.085	0.081
Eu^{3+}	0.085	0.081
Eu^{3+}	0.016	0.027
Gd^{3+}	0.015	0.027
Gd^{3+}	0.015	0.027
Gd^{3+}	0.015	0.028
Gd^{3+}	0.015	0.028
Gd^{3+}	0.04	0.012
Yb^{3+}	0.041	0.013
Yb^{3+}	0.041	0.013
Yb^{3+}	0.041	0.014
Yb^{3+}	0.042	0.013
Yb^{3+}	0.029	0.061

Table S21 The training matrix of the colorimetric response patterns against the 5 Lanthanide ions at 10 nM in river samples by using this sensor assay.

Lanthanide ions	A_i–A_0 (QA)	A_i–A_0 (TCA)
La^{3+}	0.002	-0.001
La^{3+}	-0.001	0.001
La^{3+}	-0.002	0
La^{3+}	0	-0.004
La^{3+}	0	0.001
Sm^{3+}	0.001	0.002
Sm^{3+}	-0.002	0.002
Sm^{3+}	-0.001	0.002
Sm^{3+}	0.001	-0.004
Sm^{3+}	0.002	0.002
Eu^{3+}	0.001	0.005
Eu^{3+}	-0.003	0.005
Eu^{3+}	-0.001	0.006
Eu^{3+}	0.003	0
Eu^{3+}	0.003	0.005
Gd^{3+}	0.001	0.005
Gd^{3+}	-0.003	0.005
Gd^{3+}	-0.001	0.005
Gd^{3+}	0.001	0.001
Gd^{3+}	0.002	0.006
Yb^{3+}	-0.002	0.003
Yb^{3+}	-0.006	0.003
Yb^{3+}	-0.004	0.003
Yb^{3+}	-0.002	-0.001
Yb^{3+}	-0.001	0.004